

Supporting Information

Exploration of the unusual two-step volume phase transition of the poly(*N*-vinylcaprolactam-*co*-hydroxyethyl methacrylate) hydrogel

Gehong Su,^a Liyang Jia,^a Xueqian Zhang,^a Yulin Zhang,^a Pengchi Deng,^b and Tao Zhou^{a,}*

^a State Key Laboratory of Polymer Materials Engineering of China, Polymer Research Institute,
Sichuan University, Chengdu 610065, China; ^b Analytical & Testing Center, Sichuan University,
Chengdu 610065, China

*Corresponding author. Tel.: +86-28-85402601; Fax: +86-28-85402465. E-mail address:
zhoutaopoly@scu.edu.cn (T. Zhou)

1. Theory of the scaling-MW2D spectroscopy based on auto-correlation

$W(\nu, T)$ is a $M \times N$ spectral intensity matrix. The ν and T are spectral variable (e.g., wavenumber) and perturbation variable (e.g., temperature), respectively.

$$W(\nu, T) = \begin{pmatrix} y(\nu, T_1) \\ \vdots \\ y(\nu, T_j) \\ \vdots \\ y(\nu, T_M) \end{pmatrix} \quad (1)$$

The reference spectrum and dynamic spectrum in the j th submatrix of $W(\nu, T)$:

$$\bar{y}(\nu) = \frac{1}{2m+1} \sum_{j=j-m}^{j+m} y(\nu, T_j) \quad (2)$$

$$\tilde{y}(\nu, T_j) = y(\nu, T_j) - \bar{y}(\nu) \quad (3)$$

where J corresponds to the index of rows. A mean-centered j th submatrix of $W(\nu, T)$ is obtained.

$$w_j(\nu, T) = \begin{pmatrix} \tilde{y}(\nu, T_{j-m}) \\ \vdots \\ \tilde{y}(\nu, T_j) \\ \vdots \\ \tilde{y}(\nu, T_{j+m}) \end{pmatrix} \quad (4)$$

The $w_j(\nu, T)$ has $2m+1$ rows which is called the window size. The index range of the perturbation variable I of $w_j(\nu, T)$ is from $j-m$ to $j+m$.

The generalized synchronous 2D correlation spectra is calculated from $w_j(\nu, T)$:

$$\Phi_j(\nu_1, \nu_2) = \frac{1}{2m} \sum_{j=j-m}^{j+m} \tilde{y}(\nu_1, T_j) \cdot \tilde{y}(\nu_2, T_j) \quad (5)$$

For each window, the standard deviations of spectral intensities at ν_1 and ν_2 are defined as follows.

$$\sigma(\nu_1) = \sqrt{\Phi_j(\nu_1, \nu_1)} \quad (6)$$

$$\sigma(v_2) = \sqrt{\Phi_j(v_2, v_2)} \quad (7)$$

The correlation coefficient $\rho(v_1, v_2)$ is defined:

$$\rho(v_1, v_2) = \Phi_j(v_1, v_2) / [\sigma(v_1) \cdot \sigma(v_2)] \quad (8)$$

The scaled forms of the synchronous correlation spectrum in each window are defined:

$$\Phi_j(v_1, v_2)^{(Scaled)} = \Phi_j(v_1, v_2) \cdot [\sigma(v_1) \cdot \sigma(v_2)]^{-\alpha} \cdot |\rho(v_1, v_2)|^\beta \quad (9)$$

The constant α is the scaling factor, and β is correlation enhance factor. The value of α is limited to 0–1.0.

For scaling-MW2D based on auto-correlation, the each row of the correlation matrix of scaling-MW2D is directly extracted from a diagonal line of $\Phi_j^{(Scaled)}$ matrix, namely $v_1=v_2$. Thus, the auto-correlation scaling-MW2D can be described below.

$$\Phi_j(v_1, v_1)^{(Scaled)} = \Phi_j(v_1, v_1) \cdot [\sigma(v_1) \cdot \sigma(v_1)]^{-\alpha} \cdot |\rho(v_1, v_1)|^\beta \quad (10)$$

$$\rho(v_1, v_1) = \Phi_j(v_1, v_1) / [\sigma(v_1) \cdot \sigma(v_1)] = 1 \quad (11)$$

$$\Phi_j(v_1, v_1)^{(Scaled)} = [\Phi_j(v_1, v_1)]^{1-\alpha} \quad (12)$$

The auto-correlation scaling-MW2D correlation spectrum is gained *via* sliding window position from $j=I+m$ to $M-m$ and repeating calculations of equation (2)-(12) at each window.

2. Determination of the gel content

Gel content of the resultant PVCL-co-HEMA hydrogel was measured according to the following procedure:

The newly synthesized hydrogel was dried in a vacuum oven to the constant weight, and then the hydrogel was extracted with ethanol in a Soxhlet extractor for 48 h (90 °C). After that, the extraction product was dried again to constant weight, and the gel content was calculated as

$$W_{gel} = \frac{W_d}{W_i} \times 100\%$$

where w_d is the weight of dried gel after extraction, and w_i is the initial weight of the newly synthesized gel after drying.

The gel content of the resultant PVCL-co-HEMA hydrogel in our study was measured as 82.4 wt%.

3. Determination of the VCL weight fraction in the gel

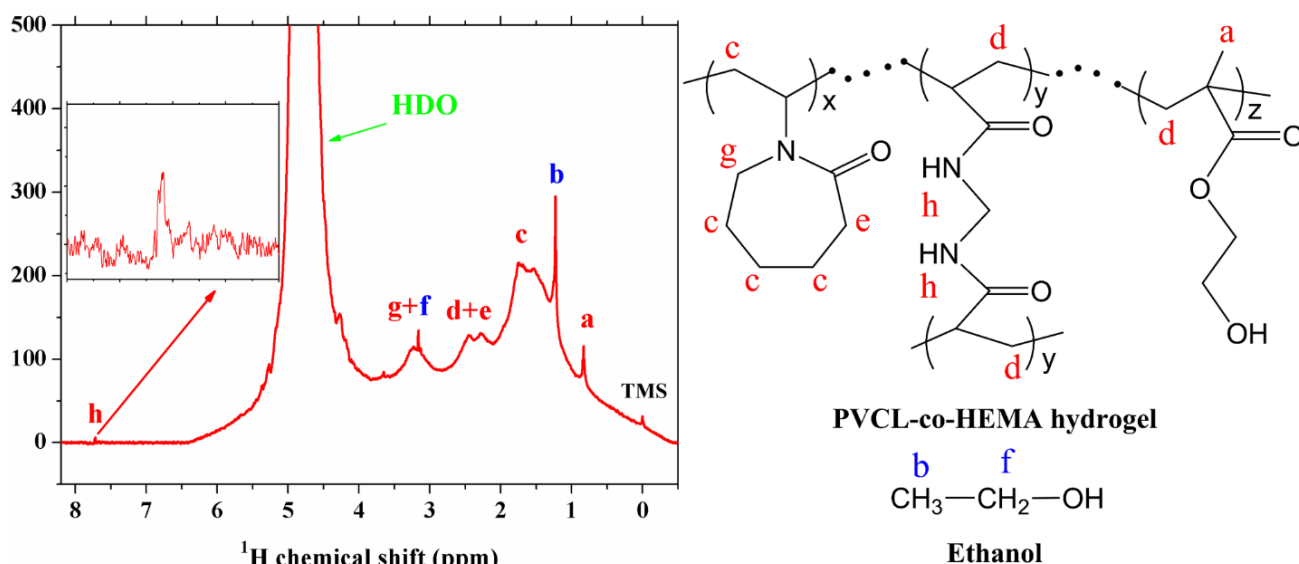


Fig. S1 ^1H HRMAS NMR spectrum of PVCL-co-HEMA hydrogel collected at 600.10 MHz.

Fig. S1 shows the ^1H HRMAS NMR spectrum of the swollen PVCL-co-HEMA hydrogel. The detailed assignments of the resonances in **Fig. S1** are summarized in **Table S1**. Based on the obtained ^1H HRMAS NMR spectrum, the molar fraction of VCL and HEMA in the resultant PVCL-co-HEMA hydrogel can be calculated:

$$x_{HEMA} = \left(\frac{A_a}{3}\right) / \left[\frac{A_c + A_{d+e} + A_{f+g} - \left(\frac{A_b}{3} \times 2\right) - A_b - \left(\frac{A_a}{3} \times 2\right) - \left(\frac{A_h}{2} \times 4\right)}{12} + \frac{A_a}{3} \right]$$

$$x_{VCL} = 1 - x_{HEMA}$$

where A represents the integral area.

Therefore, the weight fraction of VCL and HEMA in the gel can be obtained:

$$\omega_{VCL} = \frac{x_{VCL} \times M_{VCL}}{x_{VCL} \times M_{VCL} + x_{HEMA} \times M_{HEMA}} \times 100\%$$

$$\omega_{HEMA} = 1 - \omega_{VCL}$$

where M_{VCL} and M_{HEMA} represent the relative molecular mass of VCL and HEMA, respectively.

Based on these two equations, the molar fraction of VCL and HEMA in the resultant

PVCL-*co*-HEMA hydrogel was calculated as 88.6 % and 11.4 %, respectively. Besides, the weight fraction of VCL and HEMA in the gel was 89.3 % and 10.7 %, respectively.

Table S1. ^1H resonances of PVCL-*co*-HEMA hydrogel observed in **Fig. S1**

	^1H chemical shifts (ppm)	Assignment	References
a	0.83	-CH ₃ , PHEMA	1
b	1.23	-CH ₃ , ethanol	2, 3
c	1.63	-CH ₂ , PVCL	4, 5
d	2.29	-CH ₂ , PHEMA+BIS	1, 6
e	2.45	-CH ₂ , PVCL	4, 5
f	3.16	-CH ₂ , ethanol	2, 3
g	3.23	-CH ₂ , PVCL	4, 5
h	7.72	-NH, BIS	6
	4.75	HDO	7

4. Digital photographs of the Gel-2 hydrogel and the Gel-12 hydrogel

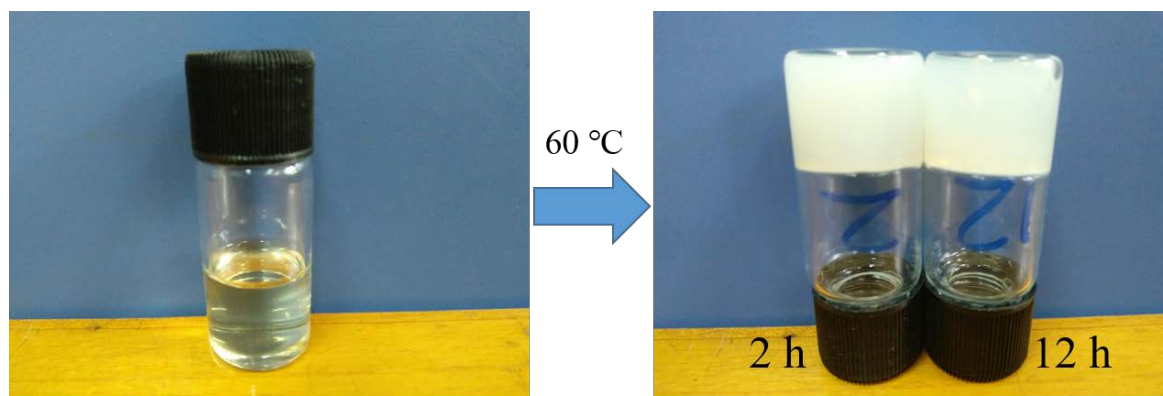


Fig. S2 Photographs of the monomer solution (left) and the resultant PVCL-*co*-HEMA hydrogels (right).

5. Second-derivative spectra in the region of C–H stretching vibration

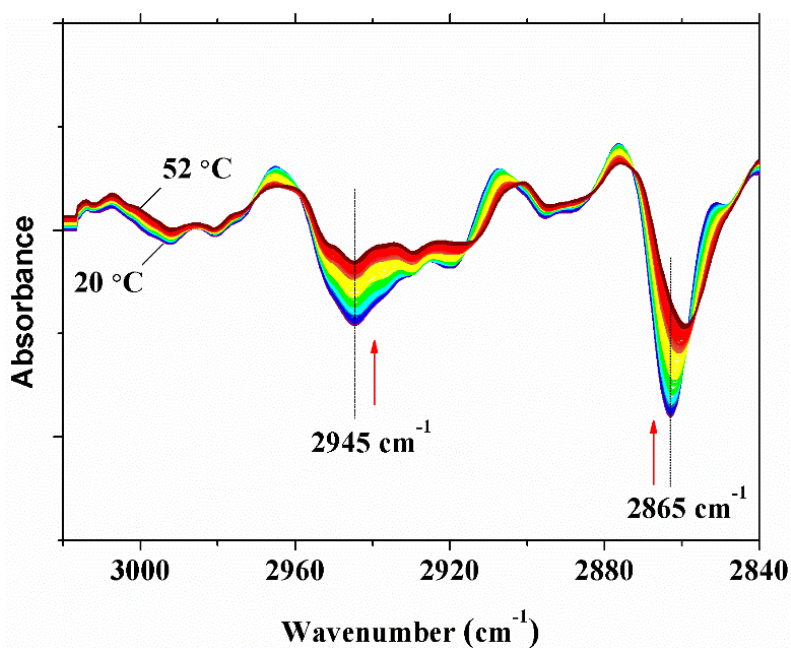
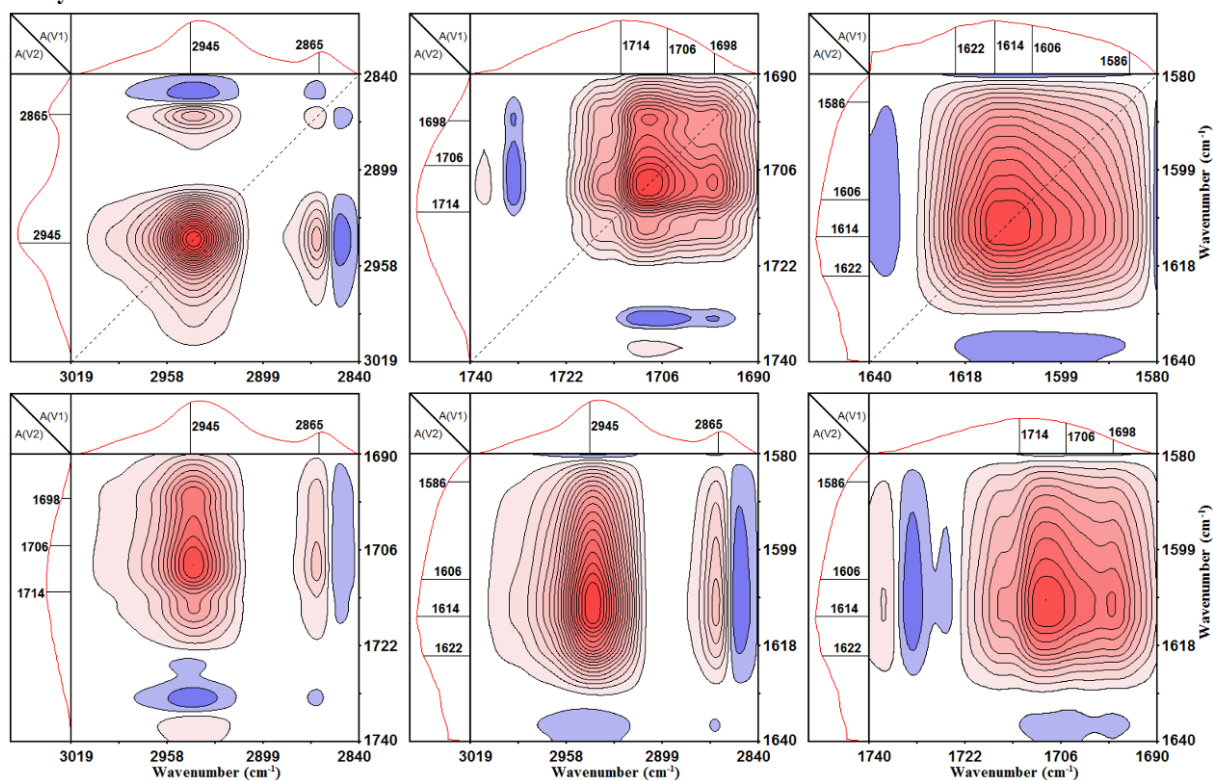


Fig. S3 Second-derivative FTIR spectra of the temperature-dependent FTIR spectra in the region of C–H stretching (3020–2840 cm^{-1}).

6. Generalized 2D correlation FTIR spectra

2D Synchronous



2D Asynchronous

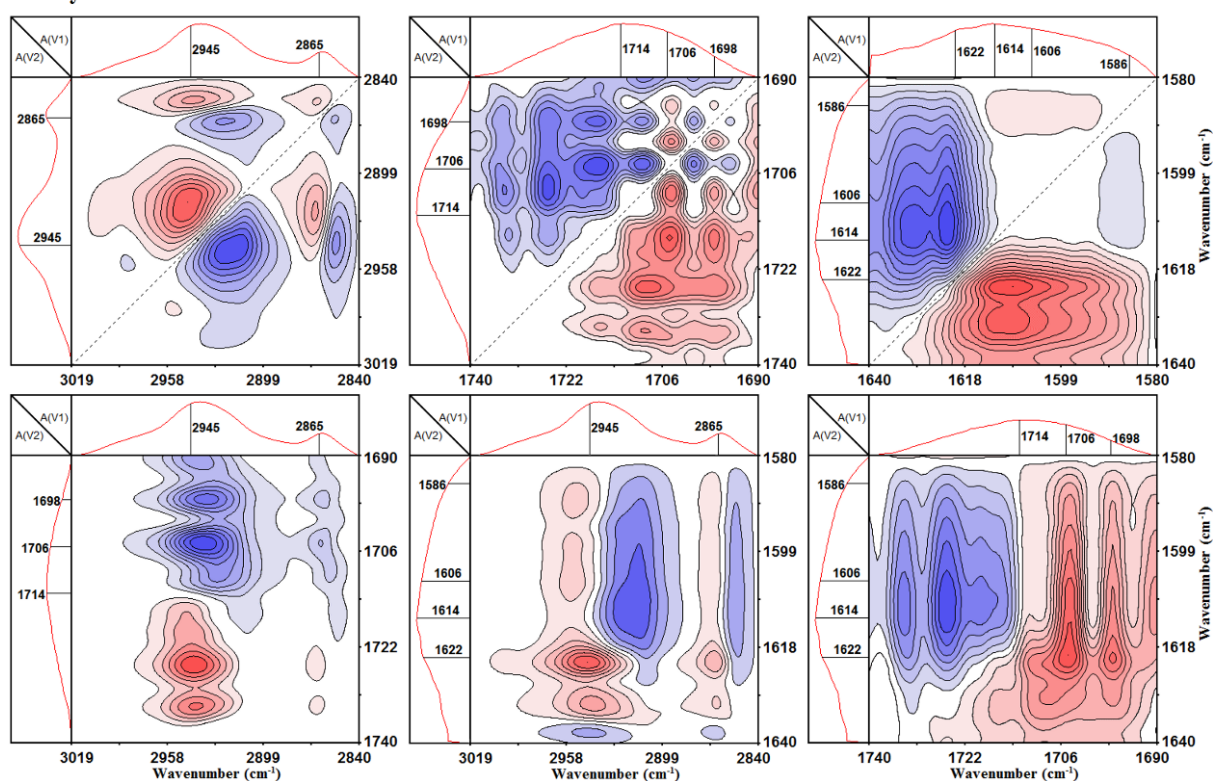
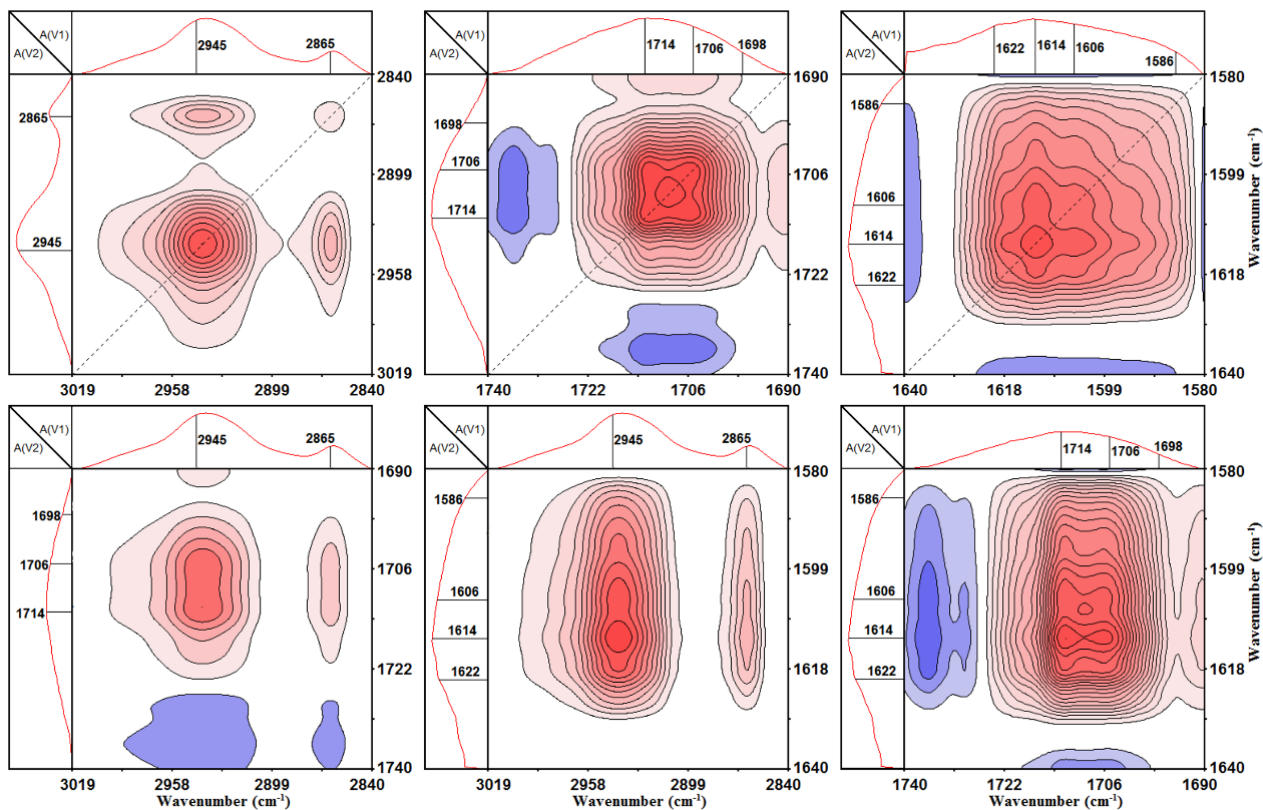


Fig. S4 Synchronous (top) and asynchronous (bottom) generalized 2D correlation FTIR spectra of PVCL-*co*-HEMA hydrogel calculated from the temperature-dependent FTIR spectra within the step I (25.0-32.3 °C). Herein, the red color is defined as positive correlation intensity, while blue color represents the negative correlation.

2D Synchronous



2D Asynchronous

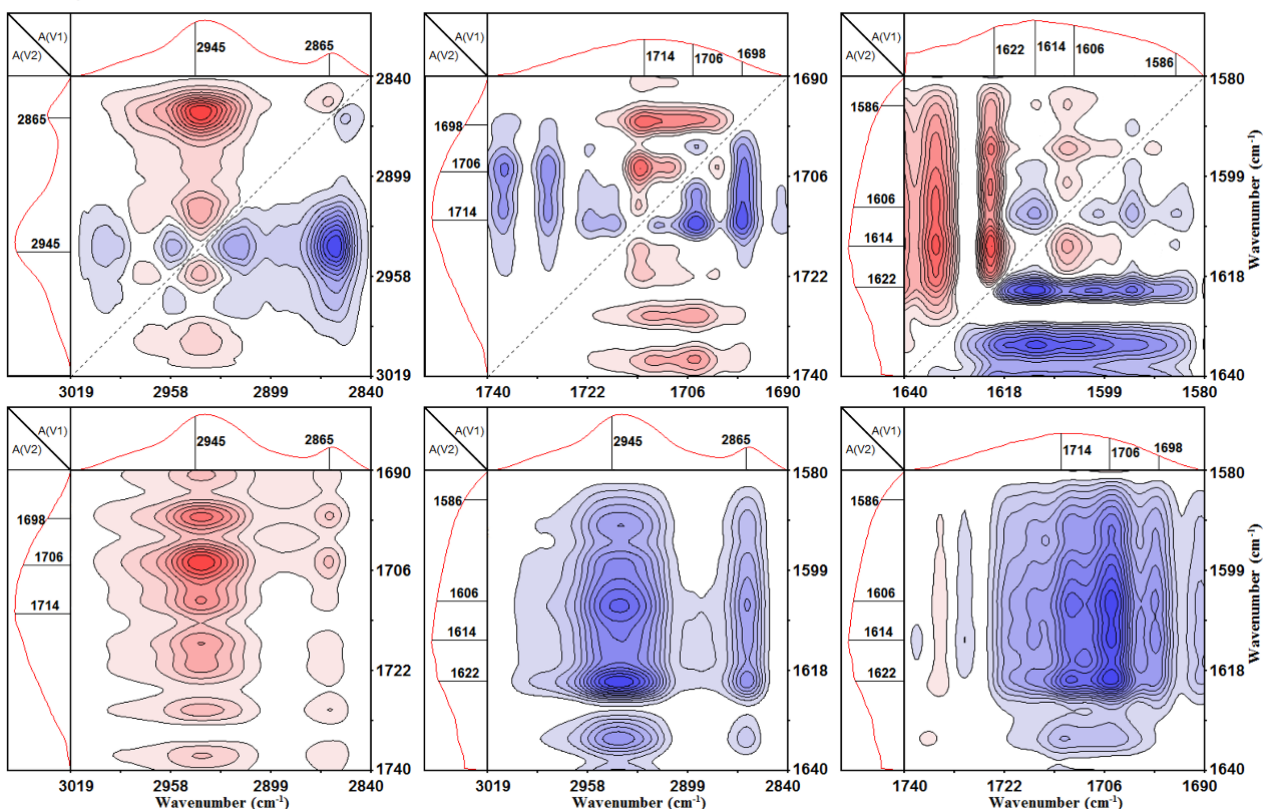


Fig. S5 Synchronous (top) and asynchronous (bottom) generalized 2D correlation FTIR spectra of PVCL-*co*-HEMA hydrogel calculated from the temperature-dependent FTIR spectra within the step II (32.3-46.8 °C).

Table S2. The sequential order of step I (25.0-32.3 °C) obtained from the synchronous and asynchronous generalized 2D correlation FTIR spectra of **Fig. S4**

Cross peaks (cm ⁻¹ , cm ⁻¹)	Synchronous	Asynchronous	Sequential order
(2945, 2865)	+	-	2865→2945
2865 cm ⁻¹ → 2945 cm ⁻¹			
(1714, 1706)	+	-	1706→1714
(1714, 1698)	+	-	1698→1714
(1706, 1698)	+	+	1706→1698
1706 cm ⁻¹ → 1698 cm ⁻¹ → 1714 cm ⁻¹			
(1622, 1614)	+	-	1614→1622
(1622, 1606)	+	-	1606→1622
(1622, 1586)	+	-	1586→1622
(1614, 1606)	+	-	1606→1614
(1614, 1586)	+	+	1614→1586
(1606, 1586)	+	+	1606→1586
1606 cm ⁻¹ → 1614 cm ⁻¹ → 1586 cm ⁻¹ → 1622 cm ⁻¹			
(2945, 1714)	+	-	1714→2945
(2945, 1706)	+	-	1706→2945
(2945, 1698)	+	-	1698→2945
(2865, 1714)	+	-	1714→2865
(2865, 1706)	+	-	1706→2865
(2865, 1698)	+	-	1698→2865
1706 cm ⁻¹ → 1698 cm ⁻¹ → 1714 cm ⁻¹ → 2865 cm ⁻¹ → 2945 cm ⁻¹			
(2945, 1622)	+	+	2945→1622
(2945, 1614)	+	+	2945→1614
(2945, 1606)	+	+	2945→1606
(2945, 1586)	+	+	2945→1586
(2865, 1622)	+	+	2865→1622
(2865, 1614)	+	+	2865→1614
(2865, 1606)	+	+	2865→1606
(2865, 1586)	+	+	2865→1586
2865 cm ⁻¹ → 2945 cm ⁻¹ → 1606 cm ⁻¹ → 1614 cm ⁻¹ → 1586 cm ⁻¹ → 1622 cm ⁻¹			
(1714, 1622)	+	+	1714→1622
(1714, 1614)	+	+	1714→1614
(1714, 1606)	+	+	1714→1606
(1714, 1586)	+	+	1714→1586
(1706, 1622)	+	+	1706→1622
(1706, 1614)	+	+	1706→1614
(1706, 1606)	+	+	1706→1606
(1706, 1586)	+	+	1706→1586
(1698, 1622)	+	+	1698→1622
(1698, 1614)	+	+	1698→1614
(1698, 1606)	+	+	1698→1606
(1698, 1586)	+	+	1698→1586

1706 cm ⁻¹ → 1698 cm ⁻¹ → 1714 cm ⁻¹ → 1606 cm ⁻¹ → 1614 cm ⁻¹ → 1586 cm ⁻¹ → 1622 cm ⁻¹
1706 cm ⁻¹ → 1698 cm ⁻¹ → 1714 cm ⁻¹ → 2865 cm ⁻¹ → 2945 cm ⁻¹ → 1606 cm ⁻¹ → 1614 cm ⁻¹ → 1586 cm ⁻¹ → 1622 cm ⁻¹

Table S3. The sequential order of step II (32.3-46.8 °C) obtained from the synchronous and asynchronous generalized 2D correlation FTIR spectra of **Fig. S5**

Cross peaks (cm ⁻¹ , cm ⁻¹)	Synchronous	Asynchronous	Sequential order
(2945, 2865)	+	+	2945→2865
2945 cm ⁻¹ → 2865 cm ⁻¹			
(1714, 1706)	+	+	1714→1706
(1714, 1698)	+	+	1714→1698
(1706, 1698)	+	+	1706→1698
1714 cm ⁻¹ → 1706 cm ⁻¹ → 1698 cm ⁻¹			
(1622, 1614)	+	+	1622→1614
(1622, 1606)	+	+	1622→1606
(1622, 1586)	+	+	1622→1586
(1614, 1606)	+	-	1606→1614
(1614, 1586)	+	+	1614→1586
(1606, 1586)	+	+	1606→1586
1622 cm ⁻¹ → 1606 cm ⁻¹ → 1614 cm ⁻¹ → 1586 cm ⁻¹			
(2945, 1714)	+	+	2945→1714
(2945, 1706)	+	+	2945→1706
(2945, 1698)	+	+	2945→1698
(2865, 1714)	+	+	2865→1714
(2865, 1706)	+	+	2865→1706
(2865, 1698)	+	+	2865→1698
2945 cm ⁻¹ → 2865 cm ⁻¹ → 1714 cm ⁻¹ → 1706 cm ⁻¹ → 1698 cm ⁻¹			
(2945, 1622)	+	-	1622→2945
(2945, 1614)	+	-	1614→2945
(2945, 1606)	+	-	1606→2945
(2945, 1586)	+	-	1586→2945
(2865, 1622)	+	-	1622→2865
(2865, 1614)	+	-	1614→2865
(2865, 1606)	+	-	1606→2865
(2865, 1586)	+	-	1586→2865
1622 cm ⁻¹ → 1606 cm ⁻¹ → 1614 cm ⁻¹ → 1586 cm ⁻¹ → 2945 cm ⁻¹ → 2865 cm ⁻¹			
(1714, 1622)	+	-	1622→1714
(1714, 1614)	+	-	1614→1714
(1714, 1606)	+	-	1606→1714
(1714, 1586)	+	-	1586→1714
(1706, 1622)	+	-	1622→1706
(1706, 1614)	+	-	1614→1706
(1706, 1606)	+	-	1606→1706
(1706, 1586)	+	-	1586→1706

(1698, 1622)	+	-	1622→1698
(1698, 1614)	+	-	1614→1698
(1698, 1606)	+	-	1606→1698
(1698, 1586)	+	-	1586→1698
$1622\text{ cm}^{-1} \rightarrow 1606\text{ cm}^{-1} \rightarrow 1614\text{ cm}^{-1} \rightarrow 1586\text{ cm}^{-1} \rightarrow 1714\text{ cm}^{-1} \rightarrow 1706\text{ cm}^{-1} \rightarrow 1698\text{ cm}^{-1}$			
$1622\text{ cm}^{-1} \rightarrow 1606\text{ cm}^{-1} \rightarrow 1614\text{ cm}^{-1} \rightarrow 1586\text{ cm}^{-1} \rightarrow 2945\text{ cm}^{-1} \rightarrow 2865\text{ cm}^{-1} \rightarrow 1714\text{ cm}^{-1} \rightarrow 1706\text{ cm}^{-1} \rightarrow 1698\text{ cm}^{-1}$			

References

1. J. V. M. Weaver, I. Bannister, K. L. Robinson, X. Bories-Azeau, S. P. Armes, M. Smallridge and P. McKenna, *Macromolecules*, 2004, **37**, 2395-2403.
2. K. Mizuno, Y. Miyashita, Y. Shindo and H. Ogawa, *J. Phys. Chem.*, 1995, **99**, 3225-3228.
3. B. Monakhova Yulia, H. Schäfer, E. Humpfer, M. Spraul, T. Kuballa and W. Lachenmeier Dirk, *Magn. Reson. Chem.*, 2011, **49**, 734-739.
4. A. Balaceanu, D. E. Demco, M. Möller and A. Pich, *Macromolecules*, 2011, **44**, 2161-2169.
5. S. Kozanoğlu, T. Özdemir and A. Usanmaz, *J. Macromol. Sci., Part A: Pure Appl. Chem.*, 2011, **48**, 467-477.
6. S. Zhang and L. Echegoyen, *J. Am. Chem. Soc.*, 2005, **127**, 2006-2011.
7. N. Wang, G. Ru, L. Wang and J. Feng, *Langmuir*, 2009, **25**, 5898-5902.